Supporting Information

End-Group Modification of Non-fullerene Acceptors Enables Efficient Organic Solar Cells

Yan Gao,[a] Qiaoling Chen,[a] Liwen Wang,[a] Hao Huang,[a] Andong Zhang,[b] Cuihong Li*,[a] Xinjun Xu[a] and Zhishan Bo*,[a,b]

[a] Beijing Key Laboratory of Energy Conversion and Storage Materials, College of Chemistry, Beijing Normal University, Beijing 100875, China

[b] College of Textiles & Clothing, State Key Laboratory of Bio-fibers and Eco-textiles, Qingdao University, Qingdao 266071, China

1. Experimental section:

Materials and synthesis

Synthesis of Compound 2.

A mixture of phenol (0.52 g, 5.52 mmol), anhydrous potassium carbonate (1.68 g, 12.19 mmol) and dry DMF (20 mL) was carefully degassed before the addition of compound **1** (1 g, 6.09 mmol). The mixture was heated to 40°C and stirred under N_2 for 16 h. After the reaction, water was added, and the mixture was extracted with ether three times. The combined organic layers were dried with $MgSO_4$, filtered and concentrated under reduced pressure. The residue was purified using silica gel chromatography eluting with DCM/petroleum ether (3:2, v/v) to afford compound **2** as a colorless solid (1.07 g, yield: 81%).^{1}H NMR (600 MHz, $CDCl_3$) δ (ppm): 7.59-7.61 (d, *J*=9.54 Hz, 1H), 7.48-7.50 (m, 2H), 7.33-7.35 (t, *J*=7.5 Hz, 1H), 7.17-7.18 (d, *J*=7.5 Hz, 1H), 7.09-7.10 (d, *J*=8.04 Hz, 2H).

Synthesis of Compound 3. To a 250 mL flask, compound **2** (1.07 g, 4.49 mmol), potassium hydroxide (5.03 g, 89.8 mmol), anhydrous ethanol (70 mL) and deionized water (70 mL) were charged subsequently. The mixture was stirred and refluxed for 24 hours. After the completion of reaction, HCl (10 mL, 5 M) was added to adjust the pH value to 1-2. The mixture was extracted with ether three times. The combined organic layers were dried with $MgSO_4$, filtered and concentrated under reduced pressure to obtain the crude compound **3** as a colorless solid in a yield of 86%. The crude product **3** was used directly in the next reaction without further purification. ^{1}H NMR (600 MHz, $CDCl_3$) δ (ppm): 9.68 (m, 2H), 7.71-7.73 (d, *J*=10.32 Hz, 1H), 7.40-7.43 (m, 2H), 7.30-7.32 (d, *J*=7.5 Hz, 1H), 7.17-7.24 (t, *J*=7.5 Hz, 1H), 7.07-7.09 (d, *J* =7.74 Hz, 2H).

Synthesis of Compound 5. A mixture of compound **3** (1.06 g, 3.84 mmol) and Ac_2O (50 mL) was refluxed overnight. After the reaction, Ac_2O was removed under reduced pressure to furnish compound **4** as a brownish yellow solid. A mixture of compound **4** (0.95 g, 3.68 mmol), trimethylamine and Ac_2O (30 mL) was carefully degassed before the addition of *tert*-butyl acetoacetate (1.16 g, 7.36 mmol). The mixture was heated at 65°C and stirred under N_2 for 12 h. After the completion of reaction, HCl (10 mL, 5 M) was added, and the mixture was heated at 85°C for 1.5 h. After cooling down to the room temperature, the mixture was extracted with DCM three times. The combined organic layers were dried with anhydrous $MgSO_4$, filtered and concentrated under reduced pressure. The residue was purified by silica gel chromatography eluting with DCM/petroleum ether (1:2, v/v) to yield compound **5** as a bright yellow solid (0.66 g, yield 70%).^{1}H NMR (600 MHz, $CDCl_3$) δ (ppm): 7.71-7.73 (d, *J*=12 Hz, 1H), 7.45-7.48 (m, 2H), 7.30-7.32 (m,

2H), 7.12-7.13 (d, *J*=6 Hz, 2H), 3.20 (s, 2H).

Synthesis of Compounds 6a and 6b. A mixture of anhydrous sodium acetate (0.63 g, 7.74 mmol), compound **5** (0.66 g, 2.58 mmol), malononitrile (0.34 g, 5.16 mmol) and absolute ethanol (30 mL) was heated to 50 °C and stirred for 3 h. Water (30 mL) was added, and the pH value of the mixture was acidified to 1-2 by aqueous HCl solution. The formed precipitate was filtered and collected. The crude product was further chromatographically purified on silica gel using DCM as an eluent to yield **6a** as a bright yellow solid (0.26 g, 33%) and **6b** as a yellow solid (0.21 g, 27%). **6a**: ^{1}H NMR (600 MHz, $CDCl_3$) δ (ppm): 8.40-8.42 (d, *J*=12 Hz, 1H), 7.47-7.50 (m, 2H), 7.32-7.35 (m, 1H), 7.26-7.28 (d, *J* =12 Hz, 1H), 7.12-7.13 (d, *J* =6 Hz, 2H), 3.67 (s, 2H)；^{13}C NMR (125 MHz, $CDCl_3$) δ 193.20, 164.35, 158.36, 156.26, 153.47, 138.27, 137.09, 130.76, 126.57, 120.42, 113.97, 112.11, 111.54, 78.11, 43.16. **6b**: ^{1}H NMR (600 MHz, $CDCl_3$) δ (ppm): 8.02-8.03 (d, *J*=6 Hz, 1H), 7.70-7.72 (d, *J* =12 Hz, 1H), 7.48-7.51 (m, 2H), 7.32-7.35 (m, 1H), 7.13-7.15 (d, *J*=12Hz, 2H), 3.68 (s, 2H); ^{13}C NMR (125 MHz, $CDCl_3$) δ192.56, 164.73, 158.71, 156.59, 153.72, 139.54, 136.29, 130.72, 126.42, 120.00, 113.72, 112.46, 111.84, 79.04, 43.22.

Synthesis of Y-G41. A mixture of compound **7** (60 mg, 0.044 mmol), **6a** (40 mg, 0.132 mmol), $CHCl_3$ (10 mL) and pyridine (0.5 mL) was heated to 45 °C and stirred under N_2 atmosphere for 12 h. The mixture was then cooled down to room temperature and evaporated to dryness under reduced pressure. The crude product was further chromatographically purified on silica gel to afford **Y-G41** as a dark blue solid (55 mg, yield 65%).^{1}H NMR (600 MHz, $CDCl_3$) δ (ppm): 9.11 (s, 2H), 8.53-8.55 (d, *J*=12 Hz, 2H), 7.47-7.50 (m, 4H), 71.31-7.37 (m, 4H), 7.16-7.18 (d, *J* =12 Hz, 4H), 4.65-4.66 (m, 4H), 3.19-3.22 (m, 4H), 2.07 (s, 2H), 1.83-1.89 (m, 4H), 1.48-1.52 (m, 4H), 1.35-1.38 (m, 4H), 1.05-1.30 (m, 52H) , 0.87-0.99 (m, 30H), 0.73-0.85 (m, 24H); ^{13}C NMR (125 MHz, $CDCl_3$) δ 186.89, 159.37, 157.80, 155.73, 154.38, 153.20, 151.77, 147.47, 144.95, 137.92, 135.26, 134.91, 134.62, 133.73, 133.01, 130.51, 130.05, 125.84, 120.54, 120.10, 115.14, 114.78, 114.32, 113.57, 112.06, 67.82, 55.59, 38.88, 31.92, 31.74, 31.21, 30.27, 29.87,29.68, 29.54, 29.36, 29.23, 25.38, 22.70, 22.59. MS (MALDI-TOF): Calcd for $C_{118}H_{114}F_2N_8O_4S_5$ (M^+): 1934.99, Found: 1935.82.

Synthesis of Y-G42. Y42 was prepared with a similar procedure to **Y-G41**. **Y-G42** was obtained as a dark blue solid (62 mg, yield 73%). ^{1}H NMR (600 MHz, $CDCl_3$) δ (ppm): 9.10 (s, 2H), 8.26-8.27 (d, *J* =6 Hz, 2H), 7.68-7.70 (d, *J*=12 Hz, 2H), 7.46-7.49 (m, 4H), 7.28-7.31 (m, 2H), 7.14-7.15 (d, *J*=6Hz, 4H), 4.75-4.76 (m, 4H), 3.19-3.22 (m, 4H), 2.12(s, 2H), 1.83-1.90 (m, 4H), 1.48-1.52(m, 4H), 1.35-1.38 (m, 4H), 1.09-1.31(m, 52H), 0.97-1.05 (m, 30H), 0.77-0.90 (m, 24H); ^{13}C NMR (125 MHz, $CDCl_3$) δ 186.49, 159.58, 158.04, 155.95, 154.65, 153.10, 151.53, 147.53, 144.94, 137.72, 136.92, 135.43, 134.58, 134.02, 133.13, 130.50, 130.34, 125.69, 120.77, 119.47, 115.29, 115.09, 114.49, 113.44, 111.89, 68.32, 55.61, 39.09, 31.93, 31.86, 31.19, 30.50, 29.87, 29.67, 29.56, 29.46, 29.35, 25.54, 22.70, 22.62. MS (MALDI-TOF): Calcd for $C_{118}H_{114}F_2N_8O_4S_5$ (M^+): 1934.99, Found: 1935.83.

Synthesis of Y-F. Y-F was synthesized with a similar method to **Y41.** ^{1}H NMR (600 MHz, $CDCl_3$) δ (ppm): 9.17(s, 2H), 8.73-8.75 (m, 0.5H), 8.40-8.42 (m, 1.5H), 7.93-7.96 (m, 1.5H), 7.57-7.59 (m, 0.5H), 7.41-7.46 (m, 2H), 4.75-4.76 (m, 4H), 3.21-3.24 (m, 4H), 2.10-2.15 (m, 2H), 1.85-1.91 (m, 4H), 1.50-1.54 (m, 4H), 1.37-1.40 (m, 4H), 1.08-1.32 (m, 52H) , 0.97-1.04 (m, 30H), 0.76-0.88 (m, 24H); ^{13}C NMR (125 MHz, $CDCl_3$) δ 187.05, 187.73, 187.28, 159.87, 159.48, 153.33, 153.49, 147.47, 145.05, 142.41, 142.43, 140.04, 139.97, 137.77, 137.67, 135.91, 135.86, 135.69, 135.34, 135.19, 134.07, 134.02, 133.32, 133.28, 133.10, 130.59, 130.52, 125.68, 125.60, 121.62, 122.44, 120.64, 120.57, 115.25, 115.11, 115.01, 114.56, 113.53, 113.49, 112.87, 112.66, 68.87, 55.63,

39.09, 31.95, 31.88, 31.87, 31.26, 30.47, 29.92, 29.80, 29.71, 29.66, 29.59, 29.58, 29.51, 29.47, 29.39, 29.37, 29.24, 25.54, 22.72, 22.64, 14.17. MS (MALDI-TOF): Calcd for $C_{106}H_{136}F_2N_8O_2S_5$ (M^+): 1750.94, Found: 1751.76.

Measurements and Instruments

^1H and ^{13}C NMR spectra were recorded on a Bruker AV 400 or 600 spectrometer. UV-visible absorption spectra were obtained on a PerkinElmer UV-vis spectrometer model Lambda 750. The electrochemical behavior of the small molecules was investigated using cyclic voltammetry (CHI 630A Electrochemical Analyzer) with a standard three-electrode electrochemical cell in a 0.1 M Bu_4NPF_6 solution in CH_3CN at room temperature under an atmosphere of nitrogen with a scanning rate of 100 mV/s. A Pt plate working electrode, a Pt wire counter electrode, and an Ag/AgCl/Cl^- reference electrode were used. The experiments were calibrated with the standard ferrocene/ferrocenium (Fc) redox system and assumption that the energy level of Fc is 4.8 eV below vacuum. MS (MALDI-TOF) measurements were performed with an Autoflex III instrument. Atomic force microscopy (AFM) measurements were performed under ambient conditions using a Digital Instrument Multimode Nanoscope IIIA operating in the tapping mode. Transmission electron microscopy (TEM) images were obtained with an FEI Tecnai TF20 transmission electron microscopy. The thickness of the blend films was determined by a Dektak 6 M surface profilometer. Hole/electron devices with structures of ITO/PEDOT:PSS (30 nm)/active layer (80 nm)/Au and ITO/ZnO (30 nm)/active layer/Ag (100 nm) are fabricated. Hole and electron mobilities of devices are calculated according to the Mott-Gurney equation $J= 9\varepsilon_o\varepsilon_r\mu V^2/8d^3$ where J is the space charge limited current, ε_o is the vacuum permittivity (ε_o = 8.85×10-12 F/m), ε_r is the permittivity of the active layer (ε_r = 3), μ is mobility, and d is the thickness of the active layer.

Grazing Incidence Wide-Angle X-ray Scattering (GIWAXS) measurements were performed at beamline 7.3.3 at the Advanced Light Source. Samples were prepared on Si substrates using identical blend solutions as those used in devices. The 10 keV X-ray beam was incident at a grazing angle of 0.12°-0.16°, selected to maximize the scattering intensity from the samples. The scattered x-rays were detected using a Dectris Pilatus 2M photon counting detector.

Solar Cells Fabrication and Characterization

OSCs were fabricated with the device configuration of ITO/ZnO (30 nm)/active layer (100 nm)/MoO_3 (8.5 nm)/Ag (100 nm). ITO glasses with a conductivity of 15Ω/square were cleaned according to the standard procedures before use. Precleaned ITO substrates were treated by UV-ozone for 20 min. A thin layer of ZnO was spin-coated on top of a cleaned ITO substrate at 3500 rpm for 15 s and annealed subsequently at 200 °C for 20 min on a hotplate before being transferred into a glove box. All solutions (6 mg mL^{-1} in 1,2-dichlorobenzene) were heated at 110 °C for at least 30 min and then spin-coated on the ZnO layer. The top electrode was thermally evaporated, with an 8.5 nm MoO_3 layer, followed by a 100 nm Ag layer at a base pressure below 10^{-7} Torr. Six cells were fabricated on one substrate with an effective area of 0.04 cm^2. The measurement of the devices was conducted in a glove box without encapsulation. The temperature while measuring the *J-V* curves was approximately 25°C.

Solubility Measurement

First, we measure the absorption maximum of three molecules of known concentration and plot it

versus solution concentration, then dilute their saturated solutions and measure the absorption maximum. According to the plotted curve, extrapolate the concentration of saturated solution and calculate the solubility.

Tables and Figures

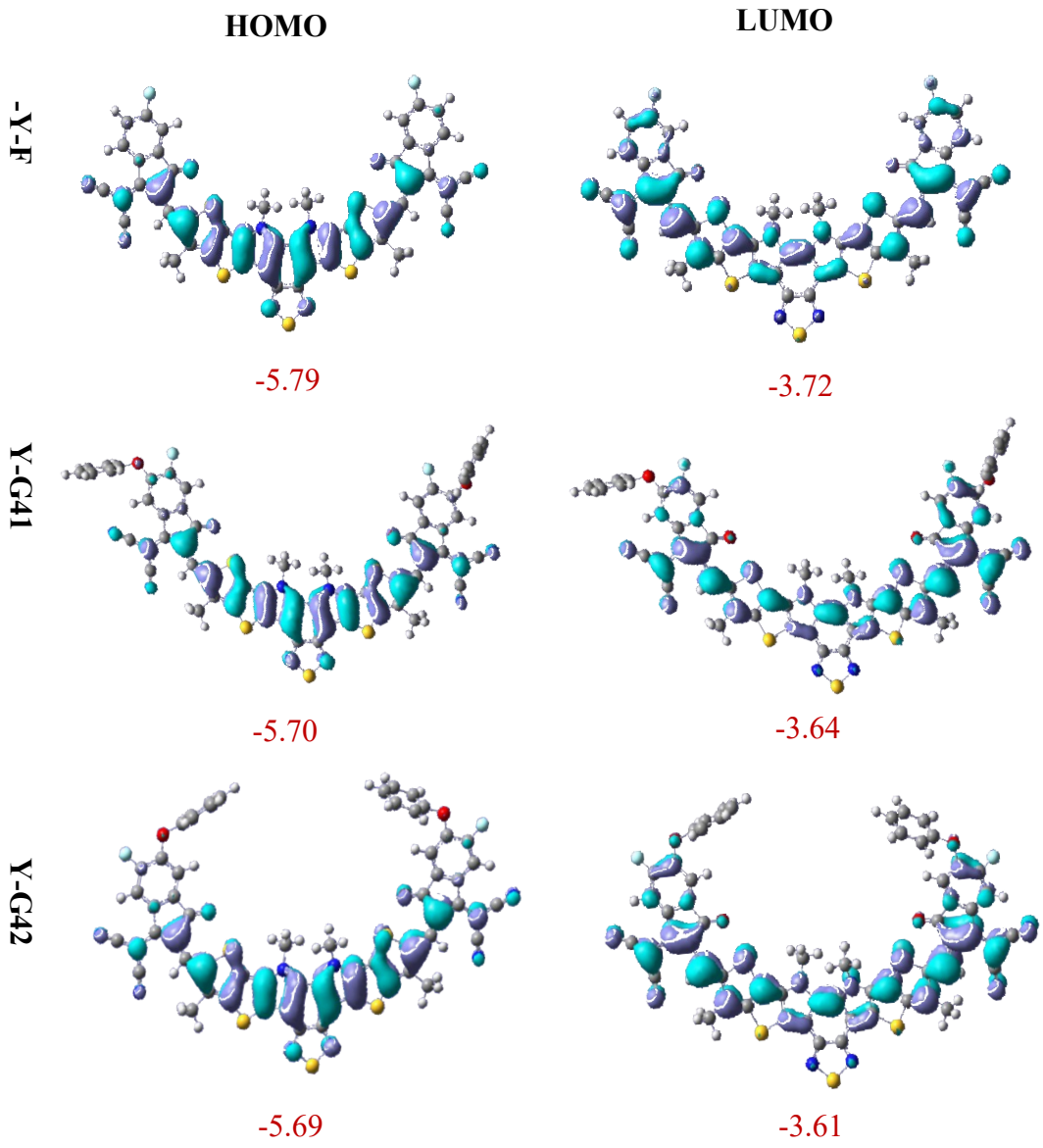

Figure S1 Frontier molecular orbitals calculated by density functional theory.

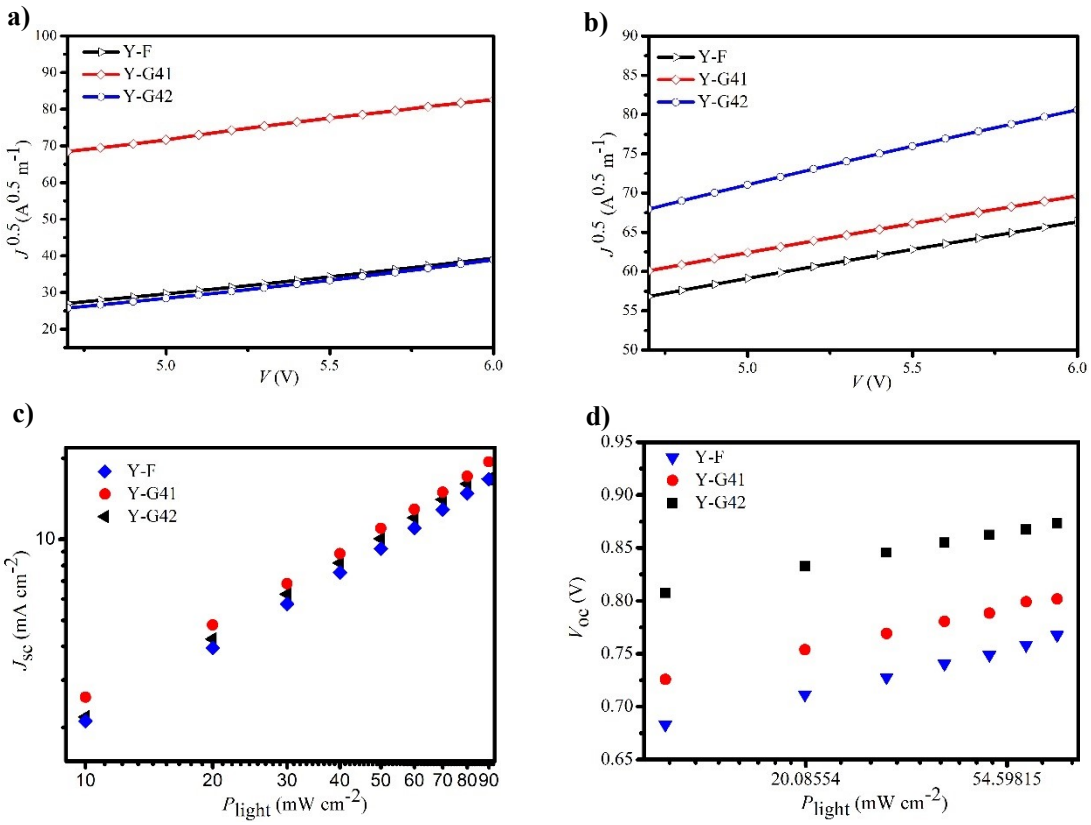

Figure S2 a) $J^{1/2}$ - V curves for determining the electron and b) hole mobilities of PBDB-T:NFAs blend films c) J_{sc} and d) V_{oc} versus light density curves of NFAs based OSCs

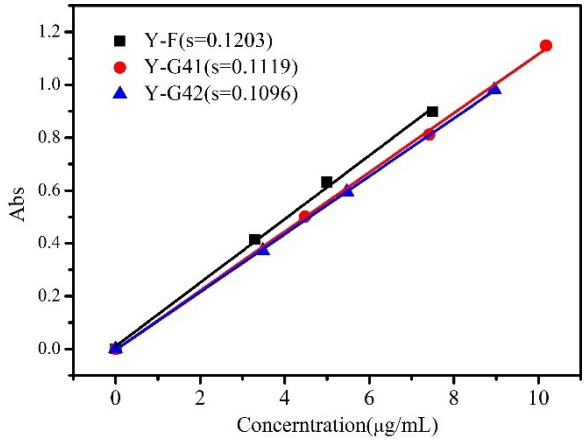

Figure S3 The calibration lines used to calculate the extinction coefficients (ε) and solubilities of the NFAs in chloroform

96.7%

98.7%

98.7%

Figure S4 Photoluminescence spectra of pure NFAs films and PBDB-T:NFAs blend film (excited at 650 nm).

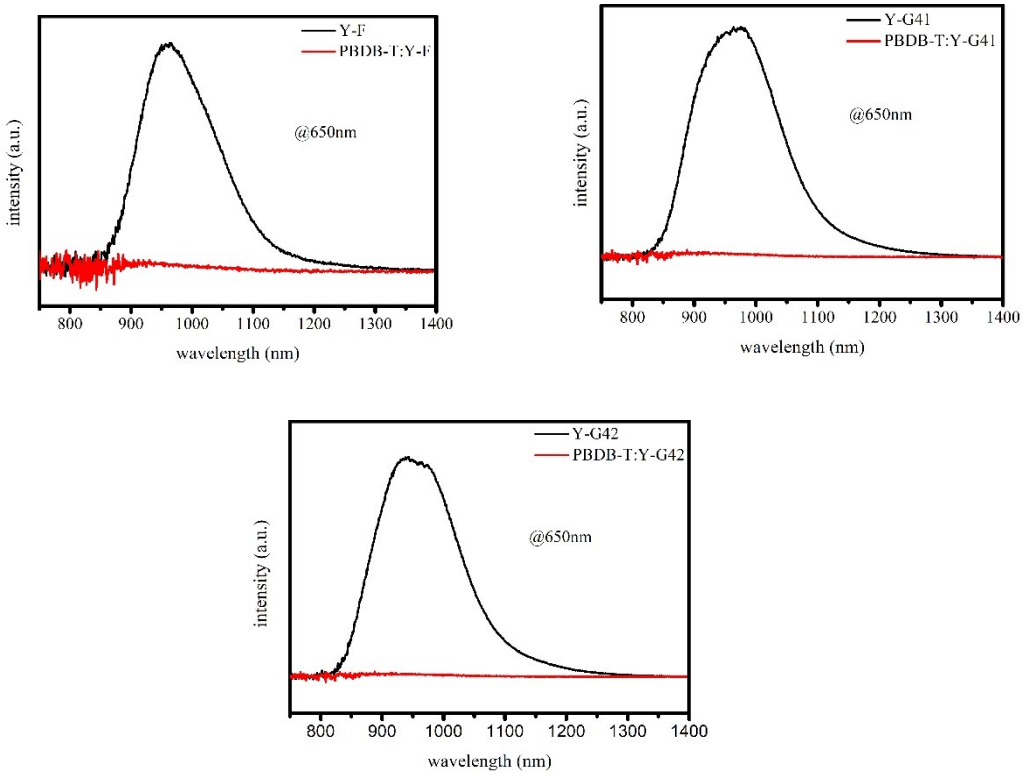

Table S1. Detailed photovoltaic parameters of PBDB-T:**Y-F** based devices processed by varied conditions.

Blends	D/A [w/w]	DIO [%]	TA [°C]	V_{oc} [V]	J_{sc} [mA cm^{-2}]	FF [%]	PCE [%]
PBDB-T:**Y-F**	1:0.8	-	-	0.84	19.17	70.37	11.12
	1:1	-	-	0.83	20.32	71.17	11.87
	1:1.2	-	-	0.84	21.45	71.02	12.53
	1:1.2	0.25	-	0.81	20.61	70.03	11.68
		0.5	-	0.80	21.48	69.66	11.95
		0.75	-	0.78	17.91	67.01	9.40
	1:1.2	-	90	0.85	20.40	67.84	11.76
		-	110	0.84	20.02	70.04	11.80
		-	130	0.82	20.21	68.20	11.32

Table S2. Detailed photovoltaic parameters of PBDB-T:**Y-G41** based devices processed by varied conditions.

Blends	D/A [w/w]	DIO [%]	TA [°C]	V_{oc} [V]	J_{sc} [mA cm^{-2}]	FF [%]	PCE [%]
PBDB-T:**Y-G41**	1:0. 8	-	-	0.86	18.43	66.20	10.35
	1:1	-	-	0.86	19.52	69.28	11.39
	1:1.2	-	-	0.87	19.96	70.14	12.12
	1:1.2	0.25	-	0.85	19.55	69.85	11.65
		0.5	-	0.85	19.06	67.85	11.06
		0.75	-	0.87	20.46	67.14	11.99
	1:1.2	-	90	0.85	18.97	68.49	11.04
		-	110	0.85	19.18	69.98	11.36
		-	130	0.84	19.50	69.04	11.31

Table S3. Detailed photovoltaic parameters of PBDB-T:**Y-G42** based devices processed by varied conditions.

Blends	D/A [w/w]	DIO [%]	TA [°C]	V_{oc} [V]	J_{sc} [mA cm^{-2}]	FF [%]	PCE [%]
PBDB-T:**Y-G42**	1:0.8	-	-	0.90	20.11	66.12	11.80
	1:1	-	-	0.91	21.17	69.12	13.08
	1:1.2	-	-	0.91	22.12	71.76	14.18
	1:1.2	0.25	-	0.89	22.09	67.90	13.35
		0.5	-	0.90	22.42	73.71	14.92
		0.75	-	0.91	23.31	72.14	15.24
	1:1.2	-	90	0.88	23.18	69.45	14.17
		-	110	0.86	23.85	68.36	14.00
		-	130	0.86	23.55	68.89	14.01
	1:1.2	0.75	90	0.87	19.74	66.63	11.42
			110	0.86	19.52	69.45	11.68
			130	0.86	19.57	68.49	11.58

Table S4. The electron mobility and hole mobility of PBDB-T:NFAs blend films.

System	μ_e (cm^2 V^{-1} S^{-1})	μ_h (cm^2 V^{-1} S^{-1})	μ_e/μ_h
PBDB-T:**Y-F**	2.91×10^{-5}	1.75×10^{-5}	1.66
PBDB-T:**Y-G41**	3.58×10^{-5}	1.76×10^{-5}	2.03
PBDB-T:**Y-G42**	3.77×10^{-5}	3.06×10^{-5}	1.23

Table S5. A summary of d-spacing and coherence lengths (CL) of the samples.

Systems	Lamellar				π–π			
	q_r [Å^{-1}]	d^a [Å]	FWHM [Å^{-1}]	CL^b [Å]	q_z [Å^{-1}]	d^a [Å]	FWHM [Å^{-1}]	CL^b [Å]
PBDB-T	0.294	21.37	0.076	73.58	1.672	3.76	0.324	17.26
Y-F	0.283	22.20	0.096	58.25	1.658	3.79	0.391	14.30
Y-G41	0.268	23.44	0.111	50.38	1.676	3.75	0.396	14.12
Y-G42	0.323	19.45	0.130	43.02	1.630	3.85	0.456	12.26
PBDB-T:Y-F	0.294	21.37	0.066	84.73	1.675	3.75	0.317	17.64
PBDB-T:Y-G41	0.293	21.44	0.076	73.58	1.677	3.75	0.322	17.37
PBDB-T:Y-G42	0.300	20.94	0.066	84.73	1.682	3.74	0.306	18.28

3. **NMR spectra**

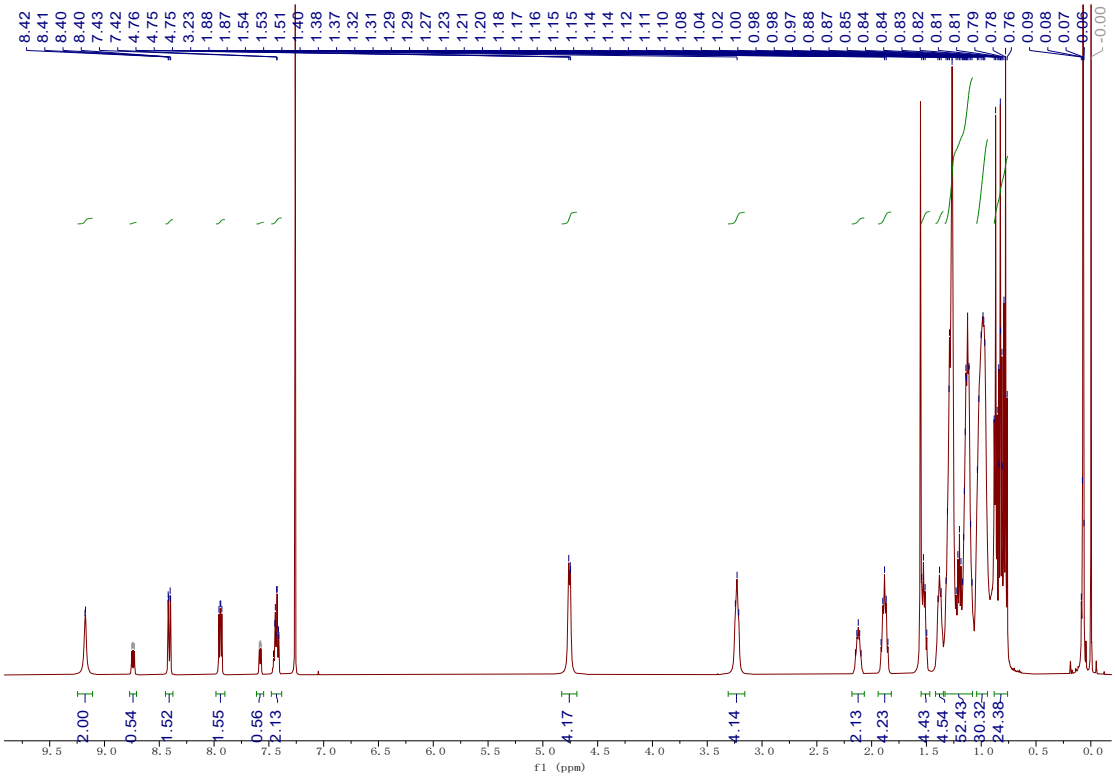

^{1}H NMR spectrum of **Y-F**

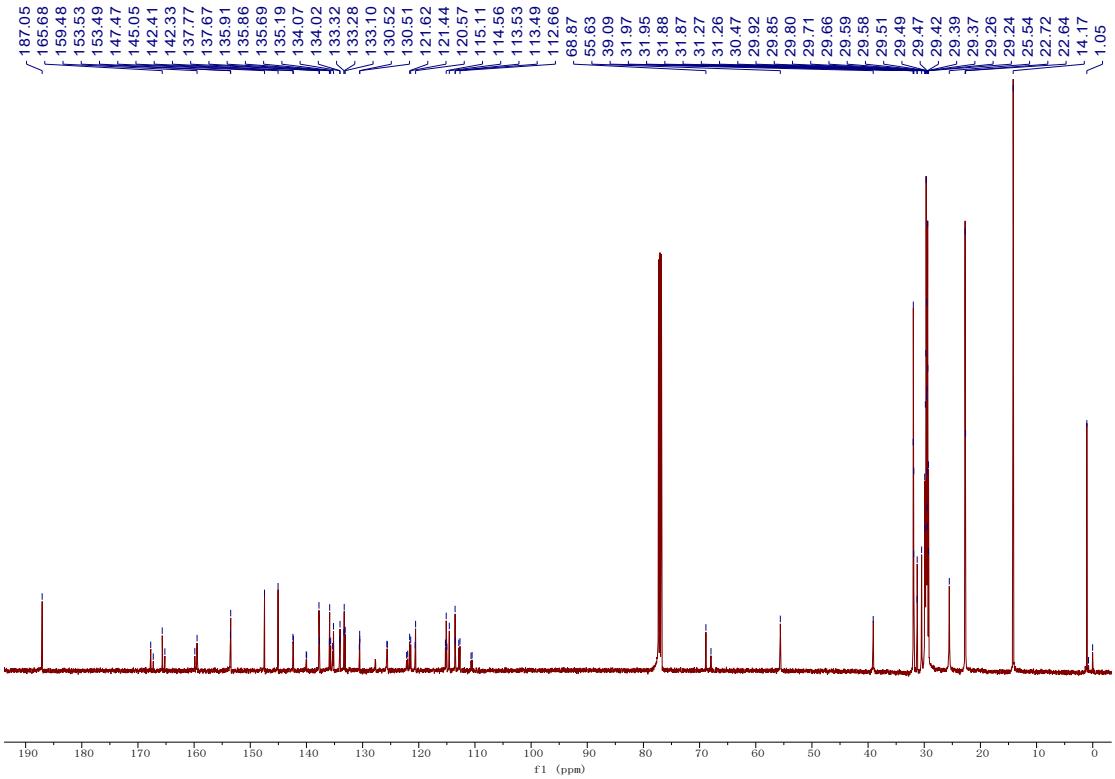

^{13}C NMR spectrum of **Y-F**

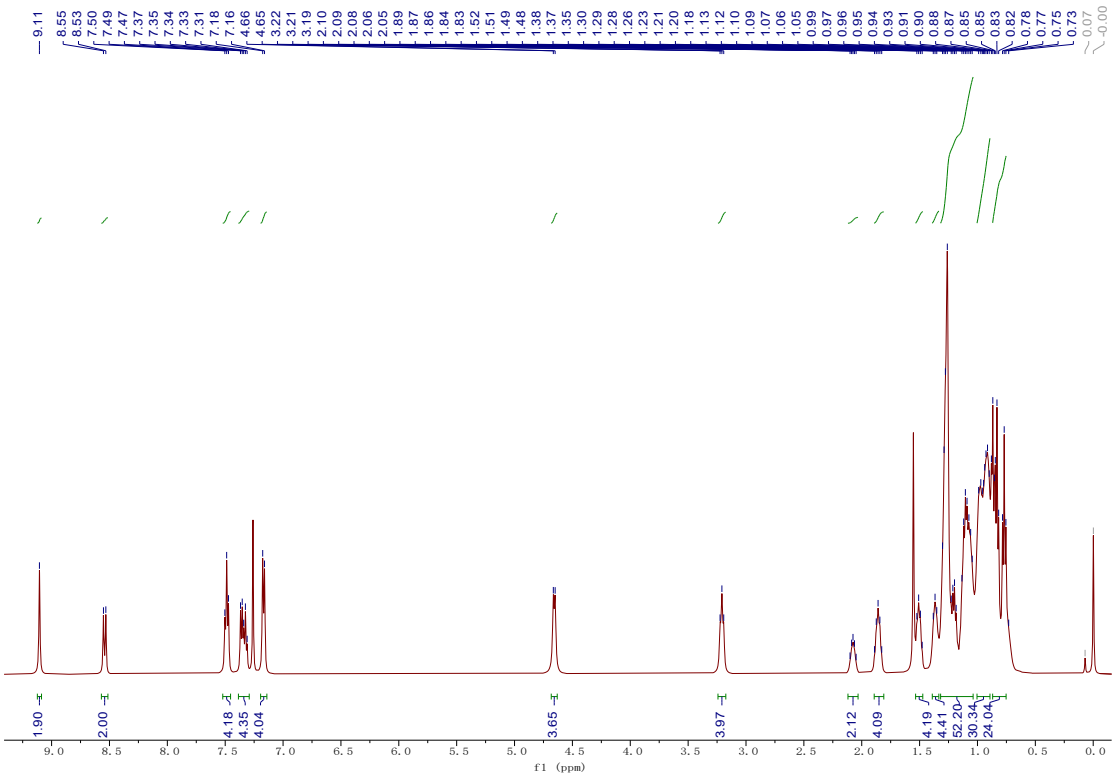

^{1}H NMR spectrum of **Y-G41**

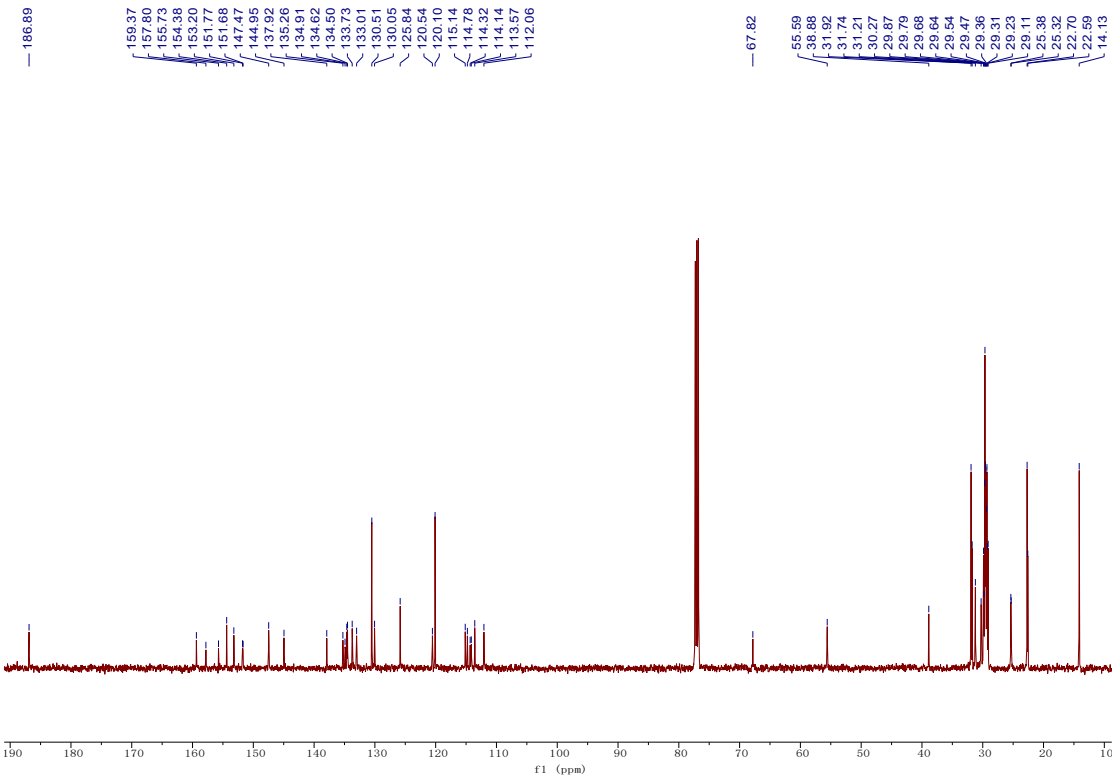

^{13}C NMR spectrum of **Y-G41**

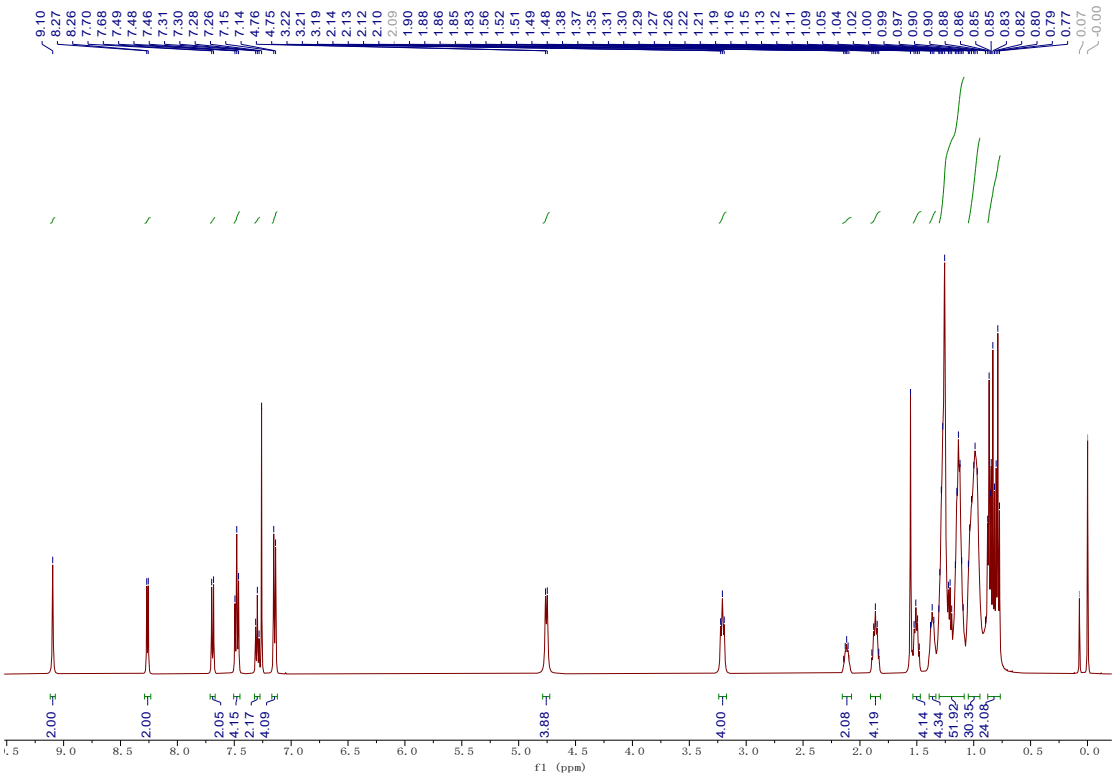

^{1}H NMR spectrum of **Y-G42**

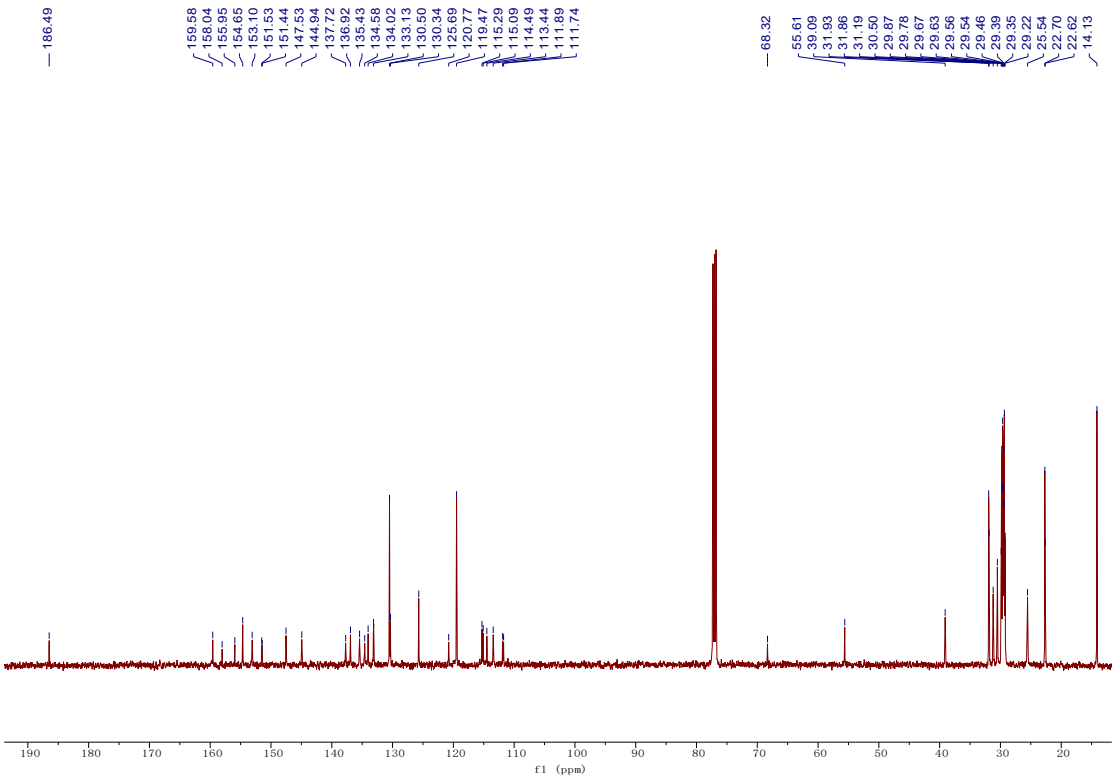

^{13}C NMR spectrum of **Y-G42**